Soft confinement of water in graphene-oxide membranes

Giovanni Romanelli [a, b, *], Andrea Liscio [c], Roberto Senesi [a, d, g], Roberto Zamboni [c], Emanuele Treossi [c], Fabiola Liscio [e], Giuliano Giambastiani [f], Vincenzo Palermo [c], Felix Fernandez-Alonso [b, h], Carla Andreani [a, d, g]

[a] Universitá degli Studi di Roma Tor Vergata, Dipartimento di Fisica and NAST Centre, Via della Ricerca Scientifica 1, 00133, Roma, Italy
[b] ISIS Facility, Rutherford Appleton Laboratory, Chilton, Didcot, Oxfordshire, OX11 0QX, United Kingdom
[c] CNR – ISOF, via Gobetti 101, Bologna, 40129, Italy
[d] CNR – IPCF Sezione di Messina, viale F. Stagno D'Alcontres 37, 98158, Messina, Italy
[e] CNR – IMM Sezione di Bologna, via Gobetti 101, Bologna, 40129, Italy
[f] CNR – ICCOM, Via Madonna del Piano 10, Sesto Fiorentino, 50019, FI, Italy
[g] Museo Storico della Fisica e Centro Studi e Ricerche Enrico Fermi, Piazza del Viminale 1, Italy
[h] Department of Physics and Astronomy, University College London, Gower Street, London, WC1E 6BT, United Kingdom

ARTICLE INFO

ABSTRACT

The spatial confinement of water in graphene-oxide membranes has been studied at room temperature using deep inelastic neutron scattering. This technique enabled the non-invasive measurement of water levels in hydrated and dried specimens, as well as of proton mean kinetic energies. For the first time, the latter observables are provided for the special case of graphene-oxide membranes. Absolute values of the mean kinetic energy provide direct insight into the local chemical environment of the proton under spatial confinement. In conjunction with parallel X-ray diffraction, atomic force microscopy, and thermal-gravimetric analysis measurements, our experimental results show that the characteristic, quasi-twodimensional confinement of water between graphene-oxide sheets results in a binding environment remarkably similar to that in the bulk. We surmise that this behaviour arises from a small fraction of hydroxyl groups relative to water molecules in graphene-oxide membranes, as well as the predominance of non-specific and weak interactions between water and the underlying nanostructured substrate.

1. Introduction

The discovery of graphene in 2004 [1] has led to the development of a new class of two-dimensional (2D) materials, and of new technologies to process them. In particular, graphene oxide (GO) can be obtained in large quantities from graphite [2,3]. The resulting sheets are characterized by very-high aspect ratios, with thicknesses of sub-nanometric dimensions and lateral sizes up to 100 μm. Unlike a perfect graphene layer having sp^2-hybridized carbon atoms arranged in a honeycomb structure, GO is a defective sheet with nanometric isolated graphenic areas surrounded by sp^3 regions containing hydroxyl, carboxyl, or epoxy groups [4,5]. The presence of these polar functional groups implies that GO can be readily dispersed in water to form stable suspensions for years. The structure of GO can be very complex and it is still hard to predict, making any extensive experimental characterization on this interesting and technologically relevant system necessary and timely. In 2011, one of the largest controversies started when a two-components model for GO was proposed [6] picturing low-oxidized graphene-like sheets to which oxidative debris strongly adhered. More recently, this model has been disputed [7] arguing that the oxidation debris are not pre-existing in all samples but are a result of a strong-base treatment during the preparation of GO.

The simple preparation and extreme 2D anisotropy enable the use of GO sheets in several applications including highly expanded porous materials [8] or self-standing membranes or powders. For these reasons, GO sheets are ideal tools to study nano-confined molecules, and studies of these processes by gas permeation or Atomic Force Microscopy (AFM) have been published recently [9]. Because of the presence of additional functional groups, GO sheets can easily restack to form lamellar GO membranes (GOMs)

displaying a remarkable stability in water as well as extraordinary mechanical properties [10]. Recent studies have shown that the gravimetric uptake of water by GO amounts to 43 wt %, and it is accompanied by an increase in interlayer distance from 5.5 Å to 8.6 Å [11]. These systems have a well-known layered structure and a large surface area (about 1000 m²/g), and represent a carbon-based hydrophilic confining environment that can accommodate water or other organic molecular species [12]. In particular, water confinement in GOMs can arise from a geometrical trapping in the layered arrangement of the GO sheets and through the chemical interaction with oxygen from epoxides.

2. Experimental

2.1. Methods

Atomic Force Microscopy (AFM) measurements were obtained in air by employing a commercial microscope Multimode III (Bruker) operating in Tapping Mode. In order to obtain a sufficiently large and detectable mechanical deflection, we used ($k = 40$ N m^{-1}) ultra-lever silicon tips (RTESPA, Bruker) with oscillating frequencies in the range between 300 and 320 KHz.

X-Ray Diffraction (XRD) measurements (out-of-plane geometry) were performed using a SmartLab-Rigaku diffractometer equipped with a rotating anode (Cu $\lambda\alpha = 1.5405$ Å), followed by a parabolic mirror to collimate the incident beam, and a series of variable slits (placed before and after the sample position).

Thermal Gravimetric Analysis (TGA) measurements were performed on an EXSTAR Thermo Gravimetric Analyzer (TG/DTA) Seiko 6200 in air (50 mL min^{-1}) coupled with a ThermoStar GSD 301T (TGA-MS) for MS gas analysis of volatile compounds.

Neutron measurements were performed at VESUVIO spectrometer (ISIS Pulsed Neutron and Muon source, UK) [13]. Samples at about 11 m from the neutron moderator where exposed to a white beam. Energies of scattered neutrons were selected through nuclear resonances with a neutron of about 5 eV absorbed by a Au nucleus and the resulting prompt gamma emission recorded by YAP detectors in the angular range 35°–70° and distances between 0.5 m and 0.7 m from the sample. The foil-cycling technique [14] was used to acquire data in the epithermal neutron region, i.e., incident energies in the range 1 eV–100 eV. Time-of-flight (t.o.f.) technique was used to evaluate energy and momentum transfers in the scattering process.

2.2. Characterization of materials

In this experimental study, two GOMs were prepared through vacuum filtration technique using GO-water suspensions (Graphene Supermarket, concentration of 6.2 g/L), further sonicated for 30 min. After sonication, suspension contained more than 95% of single-layer GO with a lateral size of 1.4 ± 0.9 μm. These structural features have been confirmed by AFM image, as shown in Fig. 1a, where GO sheets partially cover the ultraflat silicon substrate with an average thickness of 0.9 ± 0.2 nm, in agreement with the values reported in literature [15]. Elemental analysis by dynamic flash combustion indicated that the amount of Hydrogen (H) in the material is about 2 wt%, in qualitative agreement with the value reported in Refs. [16], where an approximate stoichiometry of
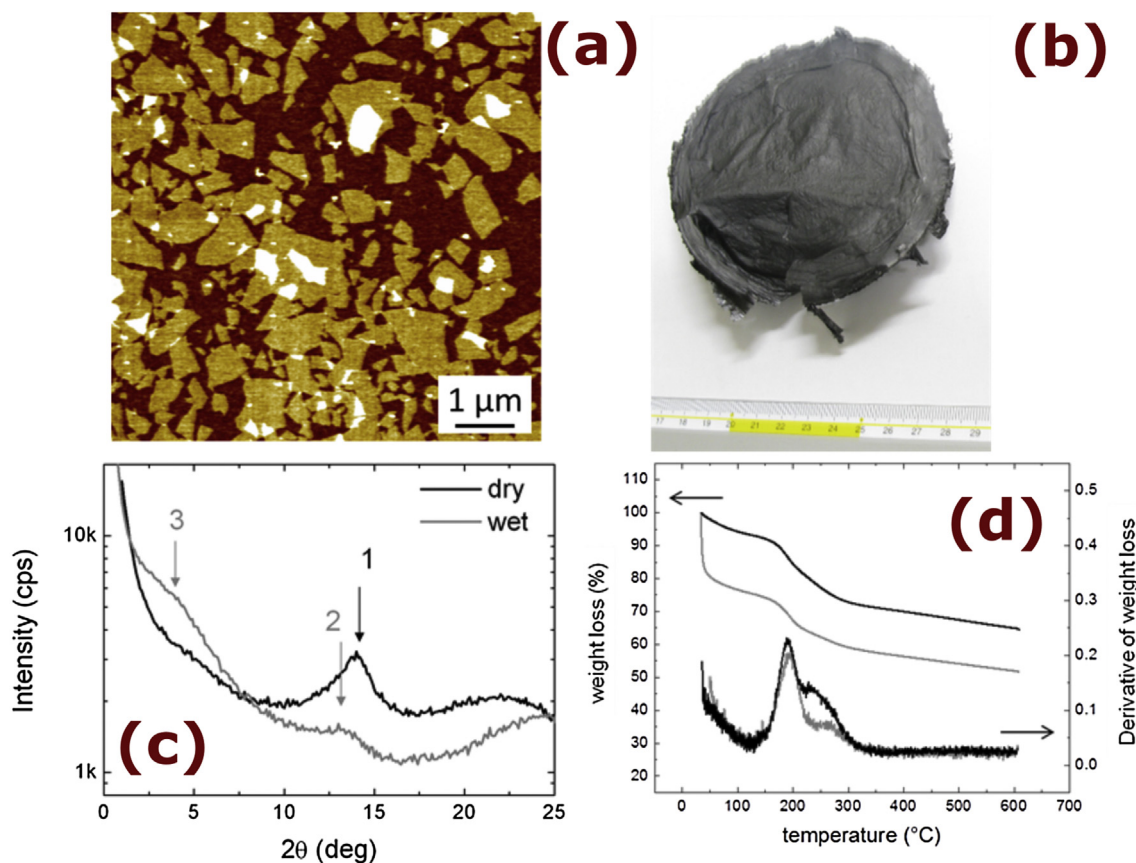

Fig. 1. (a) AFM image of the as-prepared GOM, Z-range = 3 nm; (b) As-prepared GOM before hydration; (c) XRD surveys and (d) TGA analysis of the dry (black) and hydrated (grey) membranes. (A colour version of this figure can be viewed online.)

$C_6O_3H_2$ was suggested to be compatible with either two epoxy groups and a water molecule or one epoxy group and two hydroxyls per ring [17]. The degree of oxidation amounted to a C/O ratio of 4.1 ± 0.5, as measured by X-ray Photoemission Spectroscopy. GO wettability was found to decrease for increasing oxidation values [18]. Therefore, an oxidation value larger than the average (ca. 2.4) was used to minimise the adsorption of bulk water on the GOM surface. The resulting GOMs were produced using the approach developed by Chen et al. [19], involving the evaporation of the GO suspension at 90 °C for 72 h. Each GOM was roughly circular, as shown in Fig. 1b, with a diameter and thickness of about 10 cm and 20 μm respectively, and a total mass of about 4.0 ± 0.2 g. As water was present on the surface of GOM and also trapped inside, a dedicated protocol was involved in order to reduce the amount of water adsorbed at the surface. Wet membranes for the neutron experiment were prepared under a saturated water-vapour environment for 48 h at room temperature and after left in inert atmosphere for 6 h while monitoring the weight. The measured weight decreased roughly exponentially with characteristic time of about 1 h and final stable mass of $m_{GOM, wet} = 3.42 ± 0.01$ g. The corresponding thickness of the membrane amounted to about 200 μm, being one order of magnitude larger with respect to the pristine GOM.

Dry membranes were prepared by dehydration of the pristine GOMs. Samples were heated for 12 h at 150 °C and after left in inert atmosphere for 6 h. Monitoring the weight during the thermalisation phase, the dried GOM reached the value of $m_{GOM,dry} = 1.49 ± 0.01$ g in half an hour and after it remained constant. In this case, the corresponding thickness of the membrane amounted to about 15 μm, lower than the value measured on the pristine GOM. Assuming that the two membranes adsorbed the same quantity of water at their surface, the quantity of the water trapped in the wet GOM is given by the difference between the final masses of wet and dry membranes, i.e., $m_{water} = m_{GOM,wet} - m_{GOM,dry}$, amounting to 1.93 ± 0.01 g. It is noteworthy to underline that the volume of the corresponding bulk water (ca. 1.9 ml) has the same order of magnitude as the variation in volume of the two membranes (ca. 1.5 ml), suggesting that about 20% of water is not trapped but adsorbed on the surface.

GOM is an anisotropic material with a random, in-plane distribution of holes and defects, and a periodic spacing along the graphitic *c*-axis normal to planes. As such, it may be viewed as a series of stacked GO sheets forming a multi-layered material where water can easily penetrate and be trapped. The layering of the GOM was characterized by XRD revealing an interlayer spacing of 6.3 ± 0.1 Å (peak 1 in Fig. 1c), in excellent agreement with Ref. [20].

The above results indicate that water remains trapped inside the layered structure of the dry GOM. As shown by the XRD surveys, hydration also results in the disruption of the layer stacking. The strong XRD feature at $2\theta = 14°$ decreases in intensity by about one order of magnitude (peak 2), while the scattered signal at small angles (peak 3) increases significantly corresponding to a spacing of $d_3 = 22$ Å. The latter peak can be ascribable to i) the emergence of randomly packed layers with characteristic distances d_3 as well as ii) the presence of cavities having a broad size distribution with average size d_3. Additional TGA measurements (Fig. 1d) indicate the presence of water in both dry and wet GOMs. In the case of the wet sample, about 20% of water is not trapped but adsorbed on the surface, and quickly evaporates below 70 °C. Two distinct thermal events are clearly discerned in the TGA-derivative data between 150 °C and 300 °C, indicating the presence of confined water in the GOM. At about 200–250 °C H_2O inside GOM is released as the GO layers are damaged and CO and CO_2 are released as well [21]. From this moment, a continuous and constant loss is observed together with a chemical reaction with carbon giving CO and CO_2 [22].

3. DINS experiment

Deep Inelastic Neutron Scattering (DINS) measurements [23] were performed on hydrated and dry GOMs at 27 °C using the VESUVIO spectrometer [13]. In brief, DINS is a mass-resolved and non-invasive technique that enables the measurement of absolute values of sample stoichiometry and atomic mean kinetic energies, $\langle E_K \rangle$. The latter observable provides a direct and absolute measurement of the local chemical environment around a given atomic species. Fig. 2a shows raw data as a function of scattering angle. Qualitatively, these spectra are characterized by the presence of H peaks over the t.o.f. range 125–225 μs at a scattering angle of 70° and 250–370 μs at a scattering angle of 35°, as well as (partially overlapped) C and O features in the region 350–400 μs, with small dependence on the scattering angle. Peak integrals in these data are proportional to the product of the number of atoms of a given element and the corresponding (bound) neutron-scattering cross section (largest for H). DINS data after subtraction of the sample container and summed over all front scattering directions are shown in Fig. 2b, clearly showing an increase in H levels relative to other atomic species upon hydration. Analysis of these data shows that about 40% of water in the hydrated GOM is still present in the dry sample and cannot be removed through heating *in vacuo* below 150 °C. These drying conditions represent our current limit before the structural integrity of the GOM is compromised, as shown by the TGA data in Fig. 1d.

4. Results and discussion

The width of the H peak in the raw DINS data is directly related to the square-root of $\langle E_K \rangle$. To facilitate data analysis, DINS t.o.f. data may be transformed into a momentum-space representation using standard procedures [13]. The resulting, so-called longitudinal momentum distribution for H, whose cumulative sum over all detectors, $\bar{F}(y_H)$, is shown in Fig. 2c, where y_H corresponds to the linear momentum of the H atom. The line shape of the H momentum distribution has been determined through a global fit of these data over individual detectors, in order to obtain values of $\langle E_K \rangle$ in hydrated and dry GOMs. We obtain 151 ± 7 meV and 149 ± 5 meV, respectively. In physical terms, these absolute values of the kinetic energy may be viewed as arising from inter- and intramolecular zero-point vibrations of H in water. These vibrations are a sensitive probe of the H binding environment. In bulk water at room temperature, it amounts to approximately five times the classical (equipartition) value of $3/2 k_B T \sim 35$ meV as a result of the intrinsic quantum nature of atomic motions. Recently, DINS measurements on water adsorbed in GO sponges (GOSs) where performed obtaining a value of 156 ± 2 meV [24] (additional information about the VESUVIO data reduction and analysis can be found in this work). In addition to the cases of GOMs and GOSs (hydrophilic systems), a smaller value, $\langle E_K \rangle = 144$ meV, was found for water confined in single-wall carbon nanotubes, *i.e.*, in a hydrophobic system, at T = 268 K [25]. The observed changes in the H atomic binding environment in these carbon-based systems can be determined via direct comparison to a bulk value at room temperature of $\langle E_K \rangle = 143$ meV [26]. Showing a quasi-lamellar structure, GOMs mainly display a pronounced covalent character along the GO layer corresponding to the plane normal to the confining direction and, as such, the H binding environment undergoes little disruption relative to the bulk. This result supports water's structural resilience even under these relatively stringent conditions of spatial confinement at the nanoscale. We also note that the confinement of water has also been studied in some silica-based nanostructured materials, giving indications that $\langle E_K \rangle$ for H under certain confinement conditions may attain sensibly larger values
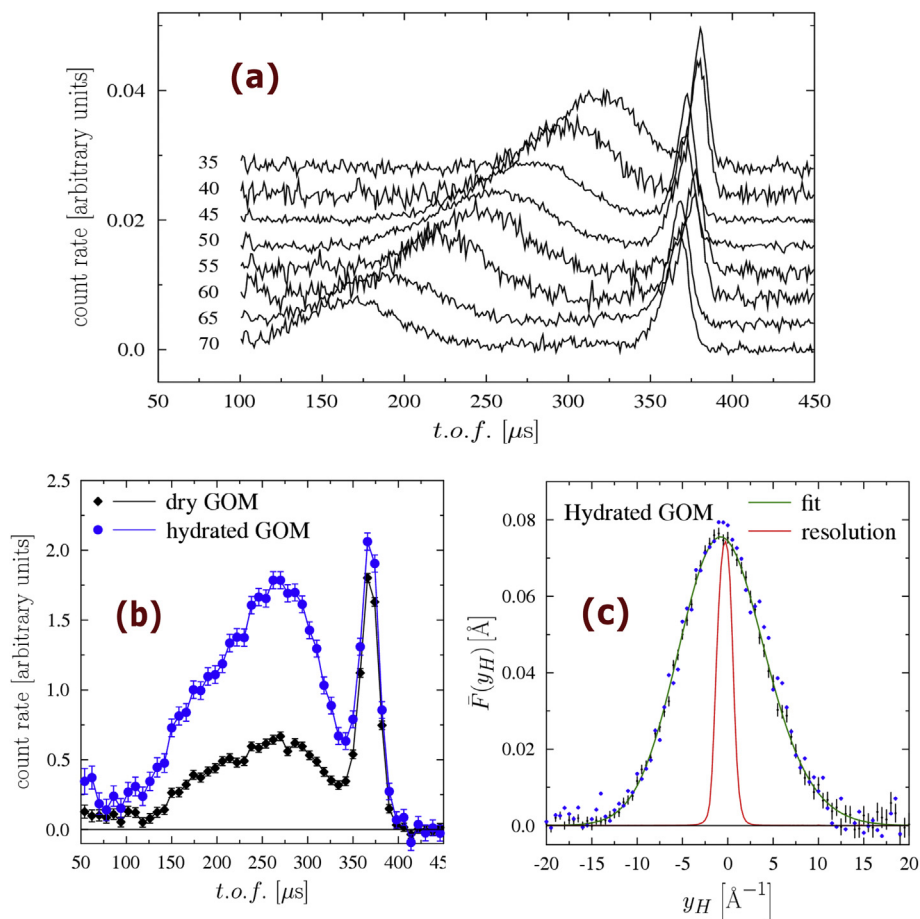
Fig. 2. (a) Raw t.o.f. data in the forward-scattering direction as a function of scattering angle in the range 35°–70°. To ease visualization, t.o.f. spectra have been shifted vertically by a constant (and arbitrary) value. (b) Raw DINS data from all forward-scattering detectors for hydrated (blue) and dry (black) GOMs after subtraction of container background. (c) H momentum distribution, $\bar{F}(y_H)$, obtained from the cumulative sum over all detectors (black error bars). The green line corresponds to a fit of the data as detailed in the main text. For reference, the resolution function of the instrument is shown in red. Blue diamonds represent the H momentum distribution in the dry sample, with error bars omitted for clarity. (A colour version of this figure can be viewed online.)

relative to the bulk [27,28], a result which is also observed for helium confined in small pores [29]. In the case of carbon-based materials and small confinement dimensions, our results to date indicate that $\langle E_K \rangle$ for H remains quite similar to bulk values, with a maximum relative increase of 9% above the bulk values for GOSs [24]. We also note that this behaviour is similar to that observed for H_2 in carbon nanotubes [30]. In the particular case of H_2, substantial departures from bulk behaviour have only been observed to date upon the intercalation of alkali-metal ions in the graphitic galleries, leading to the emergence of stronger ion-dipole and ion-quadrupole interactions between adsorbate and substrate, all of which are absent in the carbon-only precursors [31]. As was pointed out in theoretical [32] and experimental [33] studies, values of $\langle E_K \rangle$ in bulk water can vary over narrow ranges, even if changes to the shape of the momentum distribution can be observed in DINS experiments. While the present quality of the data is not sufficient to carry out a line shape analysis for H momentum distributions in GOMs, the robust value of $\langle E_K \rangle$ clearly shows that the orientationally averaged chemical local environment for H is the one characteristic for bulk phases of water and much different than what was found in silica-based confining materials [27–29]. Moreover, the fact that $\langle E_K \rangle$ for H in the dry GOMs is approximately the same as for H in bulk water is an *a posteriori* confirmation that the signal from structural H can be neglected against that from water H.

On the basis of the phenomenology presented above, water confinement in GOMs thus appears to conform to the limit of soft confinement. This behaviour may be rationalised by invoking the weaker nature of water-substrate interactions relative to those dictating bulk behaviour.

5. Conclusions

Combining different techniques such as XRD, AFM, TGA, and DINS, we have investigated the uptake and the local binding environment of aqueous protons in GOMs. Although these materials can swell adsorbing and trapping large quantities of water, DINS reveals that these conditions of strong spatial confinement do not lead to a large departure from the bulk in terms of the local binding environment of the aqueous proton. Moreover, DINS has enabled the non-invasive assessment of water-uptake levels in GOMs, a task which is hardly possible using many other analytical techniques, with few exceptions such as neutron prompt gamma analysis. From the available data on water confined in nanometric media, we find that carbon-based confining materials lead to conditions of soft or mild confinement, as attested by a modest increase in H mean kinetic energies, never exceeding 9% relative to the bulk. The experimental investigations performed so far therefore call for a more systematic characterization of the dynamics of water under extreme spatial confinement, including the use of

unique and non-invasive techniques like DINS.

Acknowledgment

References

[1] K.S. Novoselov, D. Jiang, F. Schedin, T.J. Booth, V.V. Khotkevich, S.M. Morozov, A.K. Geim, Two dimensional atomic crystals, PNAS 102 (2005) 10451–10453, http://dx.doi.org/10.1073/pnas.0502848102.

[2] V. Palermo, Not a molecule, not a polymer, not a substrate the many faces of graphene as a chemical platform, Chem. Commun. 49 (2013) 2848–2857, http://dx.doi.org/10.1039/C3CC37474B.

[3] W.S. Hummers, R.E. Offeman, Preparation of graphitic oxide, J. Am. Chem. Soc. 80 (1958) 1339, http://dx.doi.org/10.1021/ja01539a017.

[4] C. Gomez-Navarro, J.C. Meyer, R.S. Sundaram, A. Chuvilin, S. Kurasch, M. Burghard, K. Kern, U. Kaiser, Atomic structure of reduced graphene oxide, Nano Lett. 10 (2010) 1144–1148, http://dx.doi.org/10.1021/nl9031617.

[5] A. Lerf, H. He, M. Forster, J. Klinowski, Structure of graphite oxide revisited, J. Phys. Chem. B 102 (1998) 4477–4482, http://dx.doi.org/10.1021/jp9731821.

[6] J.P. Rourke, P.A. Pandey, J.J. Moore, M. Bates, I.A. Kinloch, R.J. Young, N.R. Wilson, The real graphene oxide revealed: stripping the oxidative debris from the graphene-like sheets, Angew. Chem. Int. Ed. 50 (2011) 3173–3177, http://dx.doi.org/10.1002/anie.201007520.

[7] A.M. Dimiev, T.A. Polson, Contesting the two-component structural model of graphene oxide and reexamining the chemistry of graphene oxide in basic media, Carbon 93 (2015) 544–554, http://dx.doi.org/10.1016/j.carbon.2015.05.058.

[8] Z.Y. Xia, S. Pezzini, E. Treossi, G. Giambastiani, F. Corticelli, V. Morandi, A. Zanelli, V. Bellani, V. Palermo, The exfoliation of graphene in liquids by electrochemical, chemical, and sonication-assisted techniques: a nanoscale study, Adv. Funct. Mater. 23 (2013) 4684–4693, http://dx.doi.org/10.1002/adfm.201203686.

[9] R.R. Nair, H.A. Wu, P.N. Jayaram, I.V. Grigorieva, A.K. Geim, Unimpeded permeation of water through helium-leaktight graphene based membranes, Science 335 (2012) 442–444, http://dx.doi.org/10.1126/science.1211694.

[10] C.-N. Yeh, K. Raidongia, J. Shao, Q.-H. Yang, J. Huang, On the origin of the stability of graphene oxide membranes in water, Nat. Chem. 7 (2015) 166–170, http://dx.doi.org/10.1038/nchem.2145.

[11] F. Barroso-Bujans, S. Cerveny, A. Alegrı, J. Colmenero, Sorption and desorption behavior of water and organic solvents from graphite oxide, Carbon 48 (2010) 3277–3286, http://dx.doi.org/10.1016/j.carbon.2010.05.023.

[12] F. Barroso-Bujans, F. Fernandez-Alonso, J.A. Pomposo, E. Enciso, J.L.G. Fierro, J. Colmenero, Tunable uptake of poly(ethylene oxide) by graphite-oxide-based materials, Carbon 50 (14) (2012) 5232–5241, http://dx.doi.org/10.1016/j.carbon.2012.07.008.

[13] A.G. Seel, M. Krzystyniak, F. Fernandez-Alonso, The VESUVIO spectrometer now and when? J. Phys. Conf. Ser. 571 (2014) 012006. J. Mayers, G. Reiter, The VESUVIO electron volt neutron spectrometer, Meas Sci Technol 23 (2012) 045902.

[14] E.M. Schooneveld, J. Mayers, N.J. Rhodes, A. Pietropaolo, C. Andreani, R. Senesi, G. Gorini, E. Perelli-Cippo, M. Tardocchi, Foil cycling technique for the VESUVIO spectrometer operating in the resonance detector configuration, Rev. Sci. Instrum. 77 (2006) 095103, http://dx.doi.org/10.1063/1.2349598.

[15] A. Liscio, G.P. Veronese, E. Treossi, F. Suriano, F. Rossella, V. Bellani, R. Rizzoli, P. Samorì, V. Palermo, Charge transport in graphene-polythiophene blends as studied by kelvin probe force microscopy and transistor characterization,

[16] I. Natkaniec, E.F. Sheka, K. Drużbicki, K. Hołderna-Natkaniec, S.P. Gubin, E. Yu Buslaeva, S.V. Tkachev, Computationally supported neutron scattering study of parent and chemically reduced graphene oxide, J. Phys. Chem. C 119 (2015) 18650, http://dx.doi.org/10.1021/acs.jpcc.5b01676.

[17] A. Buchsteiner, A. Lerf, J. Pieper, Water dynamics in graphite oxide investigated with neutron scattering, J. Phys. Chem. B 110 (2006) 22328, http://dx.doi.org/10.1021/jp0641132.

[18] F. Perrozzi, S. Croce, E. Treossi, V. Palermo, S. Santucci, Giulia Fioravanti, L. Ottaviano, Reduction dependent wetting properties of graphene oxide, Carbon 77 (2014) 473–480, http://dx.doi.org/10.1016/j.carbon.2014.05.052.

[19] C. Chen, Q.-H. Yang, Y. Yang, W. Lv, Y. Wen, P.-X. Hou, M. Wang, H.-M. Cheng, Self-assembled free-standing graphite oxide membrane, Adv. Mater. 21 (2009) 3007–3011, http://dx.doi.org/10.1002/adma.200803726.

[20] Y. Han, Z. Xu, C. Gao, Ultrathin graphene nanofiltration membrane for water purification, Adv. Funct. Mater. 23 (2013) 3693–3700, http://dx.doi.org/10.1002/adfm.201202601.

[21] M. Rosillo-Lopez, T.J. Lee, M. Bella, M. Harta, C.G. Salzmann, Formation and chemistry of carboxylic anhydrides at the graphene edge, RSC Adv. 5 (2015) 104198–104202, http://dx.doi.org/10.1039/C5RA23209K.

[22] M. Acik, G. Lee, C. Mattevi, A. Pirkle, R.M. Wallace, M. Chhowalla, K. Cho, Y. Chabal, The role of oxygen during thermal reduction of graphene oxide studied by infrared absorption spectroscopy, J. Phys. Chem. C 115 (2011) 19761–19781, http://dx.doi.org/10.1021/jp2052618.

[23] C. Andreani, D. Colognesi, J. Mayers, G.F. Reiter, R. Senesi, Measurement of momentum distribution of light atoms and molecules in condensed matter systems using inelastic neutron scattering, Adv. Phys. 54 (2005) 377–469, http://dx.doi.org/10.1080/00018730500403136.

[24] G. Romanelli, R. Senesi, X. Zhang, K.P. Loh, C. Andreani, Probing the effects of 2D confinement on hydrogen dynamics in water and ice adsorbed in graphene oxide sponges, Phys. Chem. Chem. Phys. 17 (2015) 31680–31684, http://dx.doi.org/10.1039/C5CP05240H.

[25] G. Reiter, C. Burnham, D. Homouz, P.M. Platzman, J. Mayers, T. Abdul-Redah, A.P. Moravsky, J.C. Li, C.-K. Loong, A.I. Kolesnikov, Anomalous behavior of proton zero point motion in water confined in carbon nanotubes, Phys. Rev. Lett. 97 (2006) 247801, http://dx.doi.org/10.1103/PhysRevLett.97.247801.

[26] C. Pantalei, A. Pietropaolo, R. Senesi, S. Imberti, C. Andreani, J. Mayers, C. Burnham, G. Reiter, Proton momentum distribution of liquid water from room temperature to the supercritical phase, Phys. Rev. Lett. 100 (2008) 177801, http://dx.doi.org/10.1103/PhysRevLett.100.177801.

[27] V. Garbuio, C. Andreani, S. Imberti, A. Pietropaolo, G.F. Reiter, R. Senesi, M.A. Ricci, Proton quantum coherence observed in water confined in silica nanopores, J. Chem. Phys. 127 (2007) 4501, http://dx.doi.org/10.1063/1.2789436.

[28] C. Pantalei, R. Senesi, C. Andreani, P. Sozzani, A. Comotti, S. Bracco, M. Beretta, P.E. Sokol, G. Reiter, Interaction of single water molecules with silanols in mesoporous silica, Phys. Chem. Chem. Phys. 13 (2011) 6022–6028, http://dx.doi.org/10.1039/C0CP02479A.

[29] C. Andreani, C. Pantalei, R. Senesi, ^{4}He adsorbed in cylindrical silica nanopores: effect of size on the single-atom mean kinetic energy, Phys. Rev. B 75 (2007) 064515, http://dx.doi.org/10.1103/PhysRevB.75.064515.

[30] D.G. Narehood, M.K. Kostov, P.C. Eklund, M.W. Cole, P.E. Sokol, Deep inelastic neutron scattering of H2 in single-walled carbon nanotubes, Phys. Rev. B 65 (2002) 233401, http://dx.doi.org/10.1103/PhysRevB.65.233401.

[31] M. Krzystyniak, M.A. Adams, A. Lovell, N.T. Skipper, S.M. Bennington, J. Mayers, F. Fernandez-Alonso, Probing the binding and spatial arrangement of molecular hydrogen in porous hosts via neutron Compton scattering, Faraday Discuss. 151 (2011) 171–197, http://dx.doi.org/10.1039/C1FD00036E.

[32] Y. Finkelstein, R. Moreh, Proton dynamics in ice VII at high pressures, J. Chem. Phys. 139 (2013) 044716, http://dx.doi.org/10.1063/1.4816630.

[33] G. Romanelli, M. Ceriotti, D.E. Manolopoulos, C. Pantalei, R. Senesi, C. Andreani, Direct measurement of competing quantum effects on the kinetic energy of heavy water upon melting, J. Phys. Chem. Lett. 4 (19) (2013) 3251–3256, http://dx.doi.org/10.1021/jz401538r.